Controlling the spectrum of single photons from triply-resonant parametric down-conversion

author, author, ...[1,2,*]

[1] *Max Planck Institute for the Science of Light, Günther-Scharowsky-Straße 1/Building 24, 90158 Erlangen, Germany*

[2] *Institute for Optics, Information and Photonics, University Erlangen-Nürnberg, Staudtstr.7/B2, 90158 Erlangen, Germany and*

[3] *SAOT, School in Advanced Optical Technologies, Paul-Gordan-Str. 6, 91052 Erlangen, Germany*

* goal: efficienct single photon atom interaction with a stable contrate and Lorentzian line profile * insdistinguishable photon pairs widely studied for non-resonant systems. * We show how PDC phase-matching temperature affects the photon spectra.

CONTENTS

I. INTRODUCTION

* efficient photon atom coupling -¿ cavity-assisted PDC -¿ Lorentzian line shape. Difficulties to lock the cavity below threshold. Additional locking lasers interfere with the detection at the single photon level -¿ extremely high suppression of the locking beam before the detectors required.

*pulsing allows to control the number of temporal modes [1]. Also exponentially rising pulses [2].

* sweep and hold technique shows the frequency mismatch of parametric down-conversion

II. SPECTRUM OF THE PARAMETRIC PHOTONS DEPENDING FREQUENCY MISMATCH

The optical resonator coupling can be described by the resonator bandwidth γ:

$$\gamma = \gamma' + \gamma'' \,. \tag{1}$$

The resonator bandwidth is the sum of the external coupling rate γ' and the internal loss rate γ'' and can be interpreted as an overall intensity decay rate of the internal resonator field. This interpretation becomes obvious in ring down spectroscopy, where a switch-off of the external pump at time $t = 0$ leads to an exponential decay of the internal field given by $|\alpha(t)|^2 = |\alpha(t=0)|^2 \cdot \mathrm{e}^{-2\pi\gamma t}$. The coupling rates γ' and γ'' are directly connected to the mirror transmittance T and the material absorption b [3]:

The resonator frequency response is then given by

$$\mathcal{G}(\nu) = 1/\left(1 - i2\left[\frac{\nu - \nu_0}{\gamma}\right]\right) = \frac{1}{1 - i2\delta} \,. \tag{2}$$

The Hamiltonian $\hat{H}$ for the three interacting fields is:

$$\hat{H} = \sum_{j \in \{\mathrm{p,s,i}\}} \hbar 2\pi\, \nu(\ell_\mathrm{j}, \mathrm{q_j}, \mathrm{p_j}) \left(\hat{a}_\mathrm{j}^\dagger \hat{a}_\mathrm{j} + 1/2\right) + \underbrace{i\hbar\pi \left(g \hat{a}_\mathrm{p} \hat{a}_\mathrm{s}^\dagger \hat{a}_\mathrm{i}^\dagger - \mathrm{h.c.}\right)}_{\equiv \hat{H}_\mathrm{I}} \,. \tag{3}$$

In the following, we consider the case of a monochromatic pump at frequency ν_p. The parametric spectum can be calculated by solving the coupled wave equations. The different frequency components of signal and idler are conveniently summarized by the frequency mismatch Δ, which is the residual mismatch between the pump electric field at frequency ν_p and the parametric resonance frequencies $\nu(\ell_\mathrm{s,i}, \mathrm{q_{s,i}}, \mathrm{p_{s,i}})$ normalized to the average bandwidth γ_si of signal and idler:

$$\Delta = \underbrace{\frac{2}{\gamma_\mathrm{s}+\gamma_\mathrm{i}}}_{=1/\gamma_\mathrm{si}} \cdot \left[\nu_\mathrm{p} - \nu(\ell_\mathrm{s}, \mathrm{q_s}, \mathrm{p_s}) - \nu(\ell_\mathrm{i}, \mathrm{q_i}, \mathrm{p_i})\right] . \tag{4}$$

For $\Delta = 0$, energy conservation allows for a maximally efficient conversion from the pump electric field frequency ν_p to the exact parametric resonance frequencies $\nu(\ell_\mathrm{s,i}, \mathrm{q_{s,i}}, \mathrm{p_{s,i}})$. In a typical experiment, the pump laser at frequency ν_p is locked to the resonance frequency of the pump mode ($\delta_\mathrm{p} = 0$) for a high intracavity power. The frequency mismatch Δ is then controlled via the temperature-dependence of the resonance frequencies $\nu(\ell_\mathrm{p,s,i}, \mathrm{q_{p,s,i}}, \mathrm{p_{p,s,i}})$.

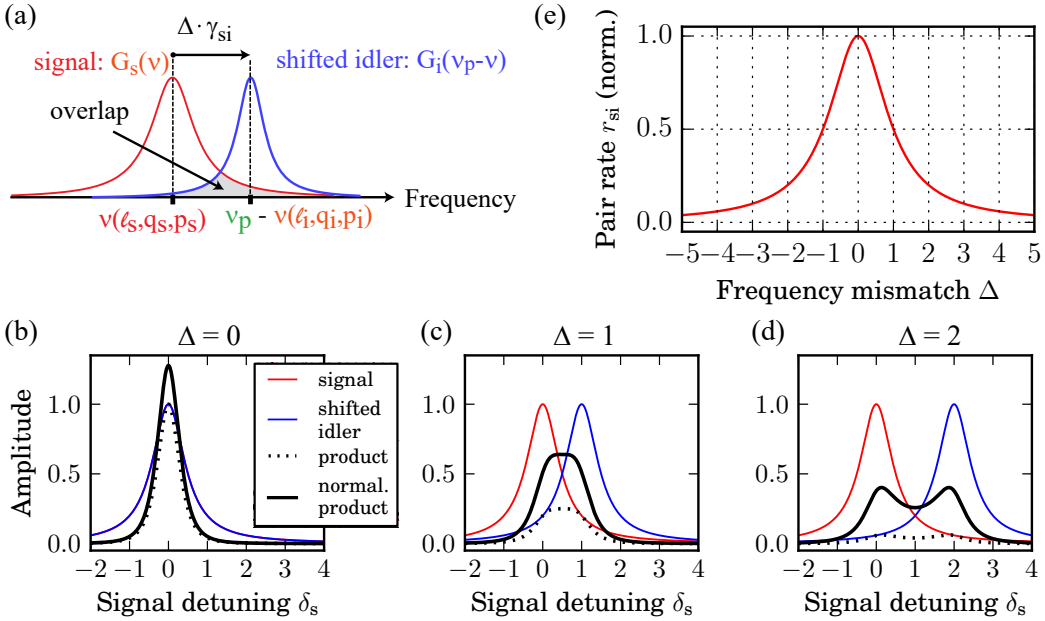

FIG. 1. Frequency spectrum of parametric down-conversion below threshold. (a) The overlap integral of the parametric response functions $\mathrm{G_{s,i}}(\nu) = |\mathcal{G}_\mathrm{s,i}(\nu)|^2$ in frequency space (see Eq. **??**) determines the parametric photon numbers $N_\mathrm{s,i}$ according to Eq. 7. (b-d) The product of the signal $\mathrm{G_s}(\nu)$ and the shifted idler $\mathrm{G_i}(\gamma_\mathrm{si}\Delta + \nu(\ell_\mathrm{s}, \mathrm{q_s}, \mathrm{p_s}) + \nu(\ell_\mathrm{i}, \mathrm{q_i}, \mathrm{p_i}) - \nu) = \mathrm{G_i}(\nu_\mathrm{p} - \nu)$ response functions ($\gamma_\mathrm{s} = \gamma_\mathrm{i} = \gamma_\mathrm{si}$ in this example) are plotted for various frequency mismatches Δ (see Eq. 4). The black line shows the product normalized to a unity area. (e) The pair production rate $r_\mathrm{si} \propto \left(1 + \Delta^2\right)^{-1}$ (see Eq. 8) as a function on the frequency mismatch Δ is Lorentzian.

The oscillation threshold for the optical pump power $P_\mathrm{th}\left(\delta_\mathrm{p}, \Delta\right)$ is then given by

$$P_\mathrm{th}\left(\delta_\mathrm{p}, \Delta\right) = \hbar 2\pi\nu_\mathrm{p}|\alpha_\mathrm{p}^\mathrm{in}|^2 = P_0 \cdot \left(1 + 4\delta_\mathrm{p}^2\right) \cdot \left(1 + \Delta^2\right) . \tag{5}$$

In the limit of low gain, i.e far below threshold, we can iteratively solve the coupled wave equation for pump, signal, and idler with first-order pertubation theory for $|\alpha_\mathrm{p} g|/\gamma_\mathrm{s,i} \ll 1$. The noise power $S_\mathrm{s,i}(\nu)$ of the parametric photons at frequency ν in the resonator follows from

$$\begin{aligned}\left\langle \hat{a}_\mathrm{s,i}^\dagger\left(\nu'\right) \cdot \hat{a}_\mathrm{s,i}\left(\nu\right)\right\rangle &= S_\mathrm{s,i}(\nu) \cdot \delta(\nu - \nu') \\ &= \frac{2}{\pi\gamma_\mathrm{s,i}} \frac{\mathrm{N_p}}{\mathrm{N_{th}}} G_\mathrm{s,i}\left(\nu + \nu(\ell_\mathrm{s,i}, \mathrm{q_{s,i}}, \mathrm{p_{s,i}})\right) G_\mathrm{i,s}\left(\gamma_\mathrm{si}\Delta + \nu(\ell_\mathrm{i,s}, \mathrm{q_{i,s}}, \mathrm{p_{i,s}}) - \nu\right) .\end{aligned} \tag{6}$$

Vacuum fluctuations[4] $\hat{\mathrm{f}}_\mathrm{i}\left(\nu\right)$ of the idler mode drive the signal noise power, and visa verse. By integrating over the

full frequency space, we get the number $N_{\mathrm{s,i}}$ of signal and idler photons in the resonator:

$$N_{\mathrm{s,i}} = \int S_{\mathrm{s,i}}(\nu)\,\mathrm{d}\nu = \frac{1}{\gamma_{\mathrm{s,i}}}\frac{\mathrm{N_p}}{\mathrm{N_{th}}}\frac{\gamma_\mathrm{s}\gamma_\mathrm{i}}{\gamma_\mathrm{si}}\frac{1}{1+\Delta^2}\,. \tag{7}$$

In parametric down-conversion, signal and idler are produced in pairs. Hence, we can define the rate of photon pair production r_si in the resonator:

$$r_\mathrm{si} = 2\pi\,\frac{\gamma_\mathrm{s}\gamma_\mathrm{i}}{\gamma_\mathrm{s}+\gamma_\mathrm{i}}\frac{P_\mathrm{p}^\mathrm{in}}{P_\mathrm{th}\,(\delta_\mathrm{p},\Delta)}\,,\quad (P_\mathrm{p}^\mathrm{in} \ll P_\mathrm{th})\,. \tag{8}$$

The simultaneous generation of signal and idler favors a description of parametric down-conversion in terms of temporal correlation functions [5–12]. The time-dependent annihilation and creation operators stem from the Fourier back-transformation $\int \mathrm{d}\nu\,\hat{a}(\nu)\,\mathrm{e}^{i2\pi\nu t} \rightarrow \hat{a}(t)$ in the the input-output formalism. The normalized cross-correlation function $\mathrm{g}_\mathrm{si}^{(2)}(\tau)$ between signal and idler in terms of the detection time difference $\tau = t_\mathrm{s} - t_\mathrm{i}$ is given by

$$\begin{aligned}\mathrm{g}_\mathrm{si}^{(2)}(\tau) &= \frac{\left\langle \hat{a}_\mathrm{s}^{\dagger\mathrm{out}}(t)\,\hat{a}_\mathrm{i}^{\dagger\mathrm{out}}(t+\tau)\,\hat{a}_\mathrm{s}^{\mathrm{out}}(t)\,\hat{a}_\mathrm{s}^{\mathrm{out}}(t+\tau)\right\rangle}{\left\langle \hat{a}_\mathrm{s}^{\dagger\mathrm{out}}(t)\,\hat{a}_\mathrm{s}^{\mathrm{out}}(t)\right\rangle\left\langle \hat{a}_\mathrm{i}^{\mathrm{out}}(t)\,\hat{a}_\mathrm{i}^{\dagger\mathrm{out}}(t)\right\rangle} \\ &= 1 + \frac{P_\mathrm{th}\,(\delta_\mathrm{p},\Delta)}{P_\mathrm{p}^\mathrm{in}}\cdot\begin{cases}\exp\left(2\pi\gamma_\mathrm{i}\tau\right) & \text{for } \tau<0\\ \exp\left(-2\pi\gamma_\mathrm{s}\tau\right) & \text{for } \tau>0\end{cases}\,.\end{aligned} \tag{9}$$

The cross-correlation is usually measured by direct detection of signal and idler.

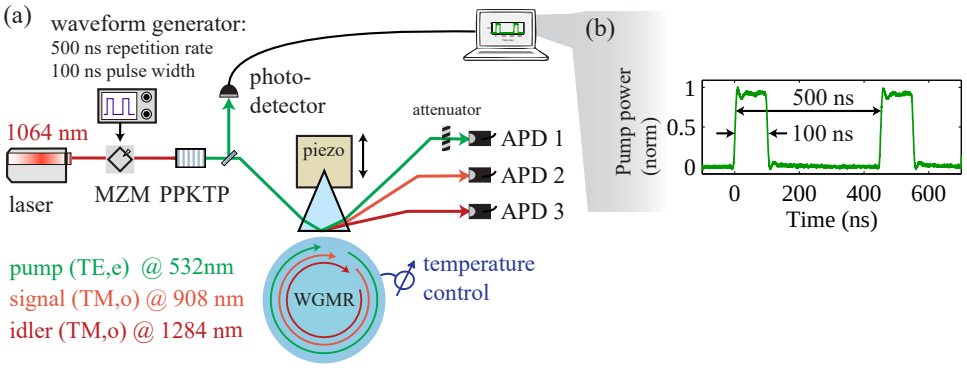

FIG. 2. Experimental setup for cavity-enhanced parametric down-conversion at pulsed excitation. (a) We use an amplitude modulator, i.e. a Mach-Zehnder modulator (MZM), to generate square pulses from a continuous wave Nd:YAG laser at a wavelength of 1064 nm. (b) The pulses are frequency-doubled in a periodically poled potassium titanyl phosphate crystal (PPKTP) and monitored on a fast photodetector before the resonator. We use avalanche photodetectors (APD) for the detection of signal and idler below threshold.

In an ideal experiment, the pump light is switched off instantaneously. The outcoupled light from the cavity then results in a peak at the end of the pulse, since there is no longer destructive interference with the directly reflected pump light. The subsequent decay of the pulse corresponds to the cavity ring-down. An exponential fit of the measured decay according to Eq. **??** gives the pump bandwidth $\gamma_\mathrm{p} = 34\,\mathrm{MHz}$, which corresponds to critical coupling of the pump mode.

In the following, we discuss the generation rate of parametric photons (see Eq. 8) depending on the phase matching of parametric down-conversion and the intracavity pump power. We show the signal count rates (see lower panels of Fig. 3(a,b)) depending on the resonator temperature. The pump laser was locked to the pump resonance at zero detuning ($\delta_\mathrm{p} = 0$). The pump laser absolute frequency then follows the temperature-induced frequency shifts[13]. This frequency shift is proportional to the frequency mismatch of parametric down-conversion given by Eq. 4.

The maximal count rates in the lower panels of Fig. 3(a,b) are achieved for a zero frequency mismatch at discrete phase matching points. The two peaks in each trace correspond to adjacent longitudinal signal modes (see Sec. **??**). The peaks become wider for the increased coupling to the resonator from Fig. 3(b) to Fig. 3(d). The non-Lorentzian

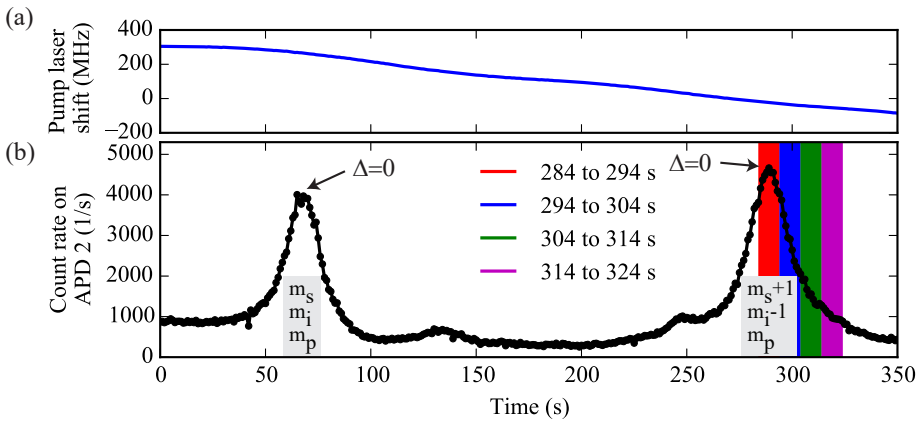

FIG. 3. Phase matching of parametric down-conversion below threshold. (a) We continuously change the frequency mismatch Δ of parametric down-conversion (see Eq. 4) on the time scale of seconds by increasing the resonator temperature. The pump laser frequency is locked to the pump mode. (b) The signal photons are detected on APD 2. The pump mode bandwidth was $\gamma_p = 16\,\mathrm{MHz}$. The single photon rates on the time scale of nanoseconds are shown in Fig. 4 for the respective frequency mismatches.

profiles (see Eq. 8) additionally indicate the presence of other conversion channels, which have not been blocked with bandpass filters for this measurement [14].

Parametric down-conversion in the resonator is driven by an exponential loading curve of the internal pump given by Eq. **??**. From an experimental point of view, the intracavity pump power at any point in time is proportional to the difference between the unmodified pump pulse (see Fig. **??**(a)) and the resonator power in the reflection port (Fig. **??**(c)[15]). The signal counts in Fig. 4 exhibit an exponential loading curve similar to the pump, but with a time constant determined by the overlap of the parametric modes depending on the frequency mismatch Δ (see Fig. **??**). The highest photon rates with the longest rise times are achieved for a zero frequency mismatch (red traces: 284 to 294 s in Fig. 4(a) and 124 to 154 s in Fig. 4(b)). At non-zero frequency mismatch Δ, photon rates are decreased and rise time is increased. We attribute the latter to the higher bandwidth of the parametric frequencies at non-zero detuning.

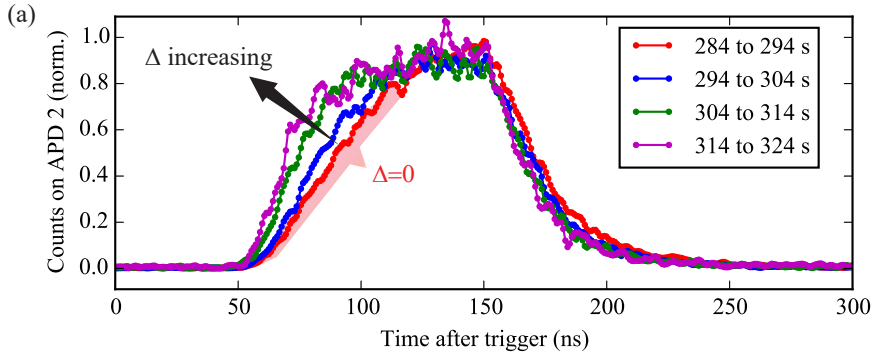

FIG. 4. Signal photon counts at pulsed excitation. Each trace corresponds to a different temperature-induced frequency mismatch Δ of parametric down-conversion shown in Fig. 3. At the beginning of the pulses, we observe shorter rise times of the count rates for an increased frequency mismatch Δ. The unmodified cavity ring-down is observed at the end of the pulses leading to a signal bandwidth of $\gamma_s = 7.4\,\mathrm{MHz}$.

At the end of the pulse, the pump light quickly couples out from the resonator. This region corresponds to the cavity ring-down where the rate of the signal photons is solely determined by the bandwidth of the signal mode. The first part of the pulse in Fig. 4 already gives us an exponentially rising single photon wave packet. The end part of the pulse, however, adds an exponentially decreasing tail to each single photon temporal mode due to cavity ring-down of each photon.

III. LOCKING THE PHASE-MATCHING TEMPERATURE

Here come figures of cavity sweeps and the shifted single photons count rate profile. The final figure is a stable lock?

IV. REFERENCES

[1] B. Brecht, K.-H. Luo, H. Herrmann, and C. Silberhorn, Applied Physics B **122**, 116 (2016).
[2] D. Sych, V. Averchenko, and G. Leuchs, in Preparation , 1 (2016), arXiv:1605.00023.
[3] H.-A. Bachor and T. C. Ralph, *A guide to experiments in quantum optics*, 2nd ed. (Wiley-VCH, 2004).
[4] For an evaluation of Eq. 6, only the term $\left\langle \hat{\mathrm{f}}_{\mathrm{s,i}}(\nu)\,\hat{\mathrm{f}}^{\dagger}_{\mathrm{s,i}}(\nu)\right\rangle = 2\pi\gamma_{\mathrm{s,i}}$ gives a non-zero contribution.
[5] J. Fekete, D. Rieländer, M. Cristiani, and H. de Riedmatten, Physical Review Letters **110**, 220502 (2013).
[6] R. J. Glauber, Physical Review **131**, 2766 (1963).
[7] M. Förtsch, J. U. Fürst, C. Wittmann, D. Strekalov, A. Aiello, M. V. Chekhova, C. Silberhorn, G. Leuchs, and C. Marquardt, Nature Communications **4**, 1818 (2013).
[8] Z. Y. Ou and Y. J. Lu, Physical Review Letters **83**, 2556 (1999).
[9] M. Scholz, L. Koch, and O. Benson, Physical Review Letters **102**, 063603 (2009).
[10] E. Bocquillon, C. Couteau, M. Razavi, R. Laflamme, and G. Weihs, Physical Review A **79**, 035801 (2009).
[11] S. Bettelli, Physical Review A **81**, 037801 (2010).
[12] K.-H. Luo, H. Herrmann, S. Krapick, B. Brecht, R. Ricken, V. Quiring, H. Suche, W. Sohler, and C. Silberhorn, (2015).
[13] The approximate proportionality factors for frequency tuning by temperature are $-27\,\mathrm{MHz\,mK^{-1}}$ for the pump mode and $-6.3\,\mathrm{MHz\,mK^{-1}}$ for the parametric modes [**?** **?**].
[14] M. Förtsch, G. Schunk, J. U. Fürst, D. Strekalov, T. Gerrits, M. J. Stevens, F. Sedlmeir, H. G. L. Schwefel, S. W. Nam, G. Leuchs, and C. Marquardt, Physical Review A **91**, 023812 (2015).
[15] Normalization is required in our case, since we used different pump powers in Fig. **??**(a) and (c).